

Influence of secant pile construction on the deformation of pile foundations in adjacent high-speed railway bridges

Changdan Wang^{1a}, Bingjun Wang^{1b}, Shunhua Zhou^{1c}, Jinglong Wang^{*1}, Xiaolong Li^{2d} and Jingjing Xu^{3e}

¹Shanghai Key Laboratory of Rail Infrastructure Durability and System Safety, Tongji University, Shanghai 201804, China

²Shanghai Donghua Local Railway Development Co., Ltd., Shanghai 200071, China

³China Railway 24th Bureau Group Co., Ltd., Shanghai 200070, China

(Received October 14, 2024, Revised January 31, 2025, Accepted February 11, 2025)

Abstract. The soil-squeezing effect induced during the construction of secant piles can significantly affect the surrounding strata and existing structures. Managing the deformation caused by secant pile construction is crucial to mitigate adverse effects. While much has been studied on the effects of secant pile construction on surrounding soil, few studies focus specifically on the deformation of high-speed railway bridge foundations in these contexts. This study integrates on-site measurements with numerical analysis. It investigates the deformation effects of secant pile construction on surrounding strata and adjacent high-speed railway bridge foundations. A finite element model was developed. The model was used to validate the feasibility of the calculation method for cylindrical cavity expansion and the equivalent simplification of three secant piles in simulating the soil-squeezing effect during construction. Based on these findings, an additional finite element model was created to assess the deformation of high-speed railway bridge piles resulting from the construction of secant piles. The model's computations considered scenarios involving secant piles constructed on single-side and on double-sides (both symmetrically and asymmetrically) of the bridge pier. This article provides insights into the impact of secant pile construction on adjacent bridge piles and offers recommendations for mitigating deformation.

Keywords: cylindrical cavity expansion; high-speed railway; numerical analysis; secant piles; soil-squeezing effect

1. Introduction

To minimize construction impact when constructing secant piles adjacent to existing structures, the preferred method generally involves driving the rotating steel casing before excavating the inner soil. However, Gao *et al.* (2019) identified significant lateral displacements particularly occurring in soft soil layers during penetration of the steel casing. This occurs because the penetrating steel casing displaces the surrounding soil outward, inducing soil movement and stress redistribution, thereby causing a soil-squeezing effect. In river excavation projects near high-speed railway piers, secant pile construction frequently occurs near existing pile foundations of railway bridges. Given the stringent requirements for controlling subgrade deformation during high-speed railway operations, comprehensive research into the deformation of existing structures caused by the secant pile forming process is essential. Studies evaluating the impact of secant pile construction on surrounding soil and adjacent structures

primarily rely on on-site tests, theoretical analysis, and numerical simulations.

Researchers widely employ on-site test and experimental test (Zhang *et al.* 2019, Mittal *et al.* 2020, Gunawan *et al.* 2022, Shan *et al.* 2023) to investigate the impact of drilling pile construction on soil deformation and adjacent structures. Shan *et al.* (2023) identified lateral extrusion deformation in surrounding strata due to steel casing bored pile construction, where the rotational process of the steel casing significantly disturbs the strata, causing substantial horizontal displacement within the depth range of the steel sleeve. Theoretical analyses (Vesić 1972, Randolph 1979, Sagaseta 1987, Rao *et al.* 2010, Liu *et al.* 2023) predominantly focus on the soil-squeezing effect induced by the rotation and downward pressure of steel casings. These studies have explored the phenomenon through methods such as cylindrical cavity expansion, providing analytical solutions for stress and displacement fields in semi-infinite soil spaces. However, theoretical analyses necessitate simplification of complex on-site conditions and appropriate assumptions to facilitate computational procedures. Numerical simulation methods, facilitated by finite element software, are also extensively employed to analyze the impact of pile construction on adjacent structure deformations (Bryson and Zapata-Medina 2010, Lueprasert *et al.* 2023, Zhou *et al.* 2023). Effective methods in numerical simulation include the displacement penetration method and the cylindrical cavity expansion method. The displacement penetration method controls displacement boundary conditions of steel casing

*Corresponding author, Ph.D. Student
E-mail: wangjinglong@tongji.edu.cn

^aPh.D.

^bM.S. Student

^cPh.D.

^dSenior engineer

^eSenior engineer

Table 1 Physical and mechanical parameters of different strata

| Strata Number | Thickness /m | Density /($\text{g}\cdot\text{cm}^{-3}$) | Compression Modulus/MPa | Cohesion/kPa | Internal friction angle/($^{\circ}$) |
|---------------|--------------|--|-------------------------|--------------|--|
| 1 | 0~10 | 1.78 | 3 | 12 | 8 |
| 2 | 0~10 | 1.91 | 5.8 | 30 | 15 |
| 3 | 0~14 | 1.95 | 7.6 | 45 | 15 |
| 4 | 0~6 | 1.88 | 8 | 15 | 24 |
| 5 | 0~10 | 2 | 12 | 90 | 18 |

components to simulate the soil-squeezing effect upon penetration into soil components. However, this process may distort the soil mesh, affecting computational efficiency and model convergence. Scholars have addressed this challenge using the ALE (Arbitrary Lagrangian-Eulerian) method and CEL (Coupled Eulerian-Lagrangian) method to achieve more accurate results (Ko *et al.* 2016, Yang *et al.* 2020, Fall *et al.* 2021). Nevertheless, these methods involve high computational costs when applied to modeling and calculating complex construction conditions, necessitating further exploration. The cylindrical cavity expansion method simulates pile formation by sequentially expanding cylindrical columns in soil layers, reflecting the soil-squeezing effect during steel casing penetration. This method is computationally efficient and yields results closely aligned with actual measurements. In scientific research, it has been noted that there is a lack of studies on the effects of secant pile construction on the deformation of nearby existing structures.

This study uses on - site tests and numerical simulations to investigate how secant pile construction impacts the deformation of nearby existing high - speed railway bridge pile foundations. Initially, monitoring points for horizontal soil displacement were placed during on - site tests to observe surrounding soil deformation during the construction of three secant piles. Subsequently, an on - site test model of secant piles was developed using ABAQUS finite element software, incorporating a simplified expansion simulation method to replicate the construction process. The model was validated against relevant monitoring results, and the feasibility of simulating the soil - squeezing effect via pile hole expansion was confirmed. Building upon this, a comprehensive finite element model was developed, incorporating secant piles, strata, and high - speed railway bridge pile foundations. The model considered scenarios where secant piles were constructed on single - side as well as on double - sides of the bridge pier, and analyzed the effects of secant pile construction on the deformation of nearby high - speed railway bridge piles under multiple conditions. These findings provide practical insights for similar engineering projects and construction designs.

2. Project overview

The river channel extension and dredging project is located in a soft soil region along the southeast coast of China. Fig. 1 illustrates the layout of the construction

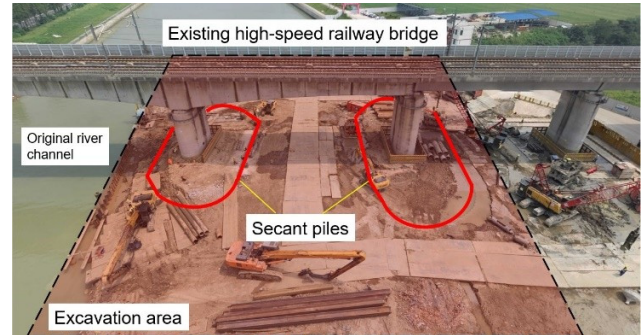


Fig. 1 The layout of the construction excavation area and the design of secant piles

excavation area and the design of secant piles. The project aims to excavate and dredge areas directly beneath an existing high-speed railway bridge, thereby expanding the current river channel to improve waterways and enhance flood discharge capacity. The primary objective is to ensure that the deformation of the existing high-speed railway bridge pile foundation in the affected area during soil excavation meets operational requirements for high-speed railways. To achieve this, secant piles will encircle the two high-speed railway bridge piers within the excavation zone, forming an island structure around them. This approach controls the deformation of bridge pile foundations by confining water within the island and managing potential foundation deformation during soil excavation outside the island. Table 1 summarizes the soil mechanical parameters obtained from the geological survey conducted at the site.

Several challenges are encountered during the construction of secant piles for the river channel extension and dredging project. Firstly, due to the project's proximity to existing high-speed railways and stringent deformation control requirements (2 mm) for bridge operations, it is crucial to monitor and control soil deformation and its impact on nearby high-speed railway bridge structures during construction activities. Secondly, the project site, located near the river channel, predominantly consists of soft soil with widespread weak strata, which may exacerbate disturbances caused by secant pile construction. To address these challenges and ensure minimal disruption to nearby high-speed railway bridge foundations, a fully-rotating full sleeve drilling rig is employed throughout the secant pile construction process. Traditional monitoring methods are utilized to maintain the verticality of steel casings and ensure adequate soil plug height inside, balancing water pressure within confined water-bearing

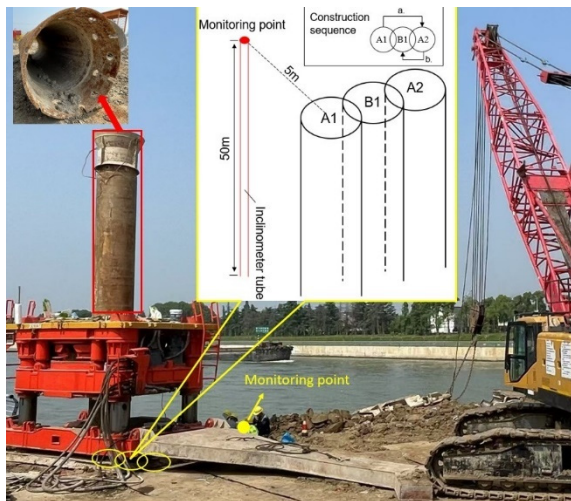


Fig. 2 Arrangement of monitoring point

sand layers to mitigate soil loss risks during grab bucket operations. Concurrently, increased monitoring of bridge pier displacement and timely adjustments to secant pile construction parameters based on monitoring feedback are implemented to facilitate smooth enclosure structure progress.

3. On-site description and test results

This section aims to examine the impact of secant pile construction on surrounding soil deformation and to provide data for validating the accuracy of numerical models. To achieve this, soil horizontal displacement monitoring equipment was deployed around the trial pile construction area to analyze the effects of secant pile construction on soil deformation.

3.1 On-site description

To clarify the construction process of secant piles and evaluate their impact on soil deformation, three secant piles were chosen for the on-site test. Soil horizontal displacement monitoring equipment was positioned 5 meters away from the test pile location. The piles were built sequentially as A1→A2→B1, each measuring 43.0 m in length and 1.0 m in diameter. The center-to-center distance between each secant pile was 0.8 m. Horizontal soil displacement was monitored to a depth of 0-50 meters. Fig. 2 illustrates the layout of the on-site test and the construction sequence of secant piles.

3.2 On-site test results

The monitoring results of horizontal soil displacement at measurement points is presented in Fig. 3. In these results, soil displacement towards the secant piles side is denoted as positive (+), while displacement in the opposite direction is negative (-). Analysis reveals significant lateral soil squeezing effects in the surrounding area during secant pile construction in soft soil. As construction progresses, the

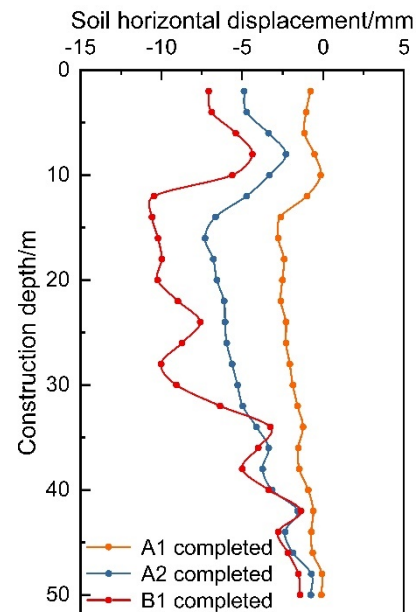


Fig. 3 On-site test results

trend of horizontal soil displacement remains consistent. Specifically, following the construction of the A1 pile, a maximum horizontal displacement of -2.8 mm occurred at a depth of 16.0 m. After the A2 pile construction, this displacement increased to -7.3 mm at the same depth, and after the B1 pile construction, it reached a maximum of -10.6 mm at 14.0 m depth. Significant soil displacement primarily occurred within the 14.0 to 16.0 m depth range, with the A2 pile causing an incremental displacement of 4.5 mm and the B1 pile causing 3.3 mm. Notably, the construction of B1 induced a comparatively smaller displacement increment. These monitored data suggest that constructing secant pile enclosure structures adjacent to existing high-speed railway structures in soft soil may unexpectedly deform the underlying high-speed railway bridge pile foundation, potentially jeopardizing train safety.

4. Model of secant pile construction

To further investigate the impact of secant pile construction on adjacent high-speed railway bridge pile foundations, the ABAQUS software was used to establish a three-dimensional numerical model of secant piles interacting with the stratum. The model aims to investigate the effects of the cylindrical cavity expansion method and simplified equivalent expansion methods (three secant piles) in simulating the soil-squeezing effects induced by construction activities, validated against on-site test results.

4.1 Secant piles-stratum model

a) Structural parameters and boundary conditions

The soil model for the on-site test measures 30 m in length, 30 m in width, and 50 m in height. The dimensions of the secant pile are strictly based on actual site parameters, with cylindrical cavity expansions positioned

Table 2 Summary of soil parameters

| Strata Number | Thickness /m | Element Type | Density /($\text{g}\cdot\text{cm}^{-3}$) | Elastic Modulus/MPa | Poisson's ratio |
|---------------|--------------|---------------|--|---------------------|-----------------|
| 1 | 10 | Solid Element | 1.78 | 10.5 | 0.35 |
| 2 | 10 | | 1.91 | 20.3 | 0.35 |
| 3 | 12 | | 1.95 | 28 | 0.35 |
| 4 | 8 | | 1.88 | 30 | 0.3 |
| 5 | 10 | | 2 | 42 | 0.3 |

Table 3 Parameters of secant piles

| Length/m | Internal diameter/m | External diameter/m | Element Type | Density /($\text{g}\cdot\text{cm}^{-3}$) | Elastic Modulus/MPa | Poisson's ratio |
|----------|---------------------|---------------------|---------------|--|---------------------|-----------------|
| 43 | 1.00 | 1.08 | Solid Element | 2.5 | 30 | 0.2 |

centrally within the soil. Boundary conditions define the model's upper surface as free, controlling horizontal displacement at the model sides and both horizontal and vertical displacements at the bottom surface. To enhance computational efficiency, each layer of soil is modeled as a uniform material, with its thickness set according to the maximum value, based on geological exploration and relevant soil parameters.

b) Material parameters

Solid elements are employed for all components, with soil modeled using Mohr-Coulomb yield conditions. The secant pile utilizes a linear elastic model. Material parameters for each soil layer are detailed in Table 2, while secant pile parameters are provided in Table 3.

c) Contact and load settings

Surface-to-surface contact is established between the secant piles and the soil in this analysis. The normal contact between these surfaces is considered as hard contact, while in the tangential direction, a penalty function contact algorithm is employed with a friction coefficient set at 0.3. The gravitational field is uniformly applied across the entire model area, and displacement boundary conditions are imposed on the outer surface of the secant pile to ensure consistent radial expansion.

d) Simulation method for secant pile construction

The simulation of soil-squeezing effects from secant pile construction in finite element software utilizes the cylindrical cavity expansion method in this study. This method (shown in Fig. 4(a)) sequentially applies displacement conditions to cylindrical components embedded in the soil, expanding their lateral surfaces from an initial radius D_0 to a final radius D_u , thus simulating soil-squeezing effects during steel casings pressing. Drawing from literature (Shan *et al.* 2023), this study assumes that during the insertion of steel casings into the formation, a certain volume of soil is squeezed out from the casing. Assuming the soil remains uncompressed throughout this process, the volume of soil displaced should theoretically equal the volume of the steel casing pressed in. With a steel casing thickness of 0.04 m on site, D_0 is set at 0.5 m and D_u at 0.54 m. The cylindrical cavity expansion method involves dividing cylindrical components along the depth of

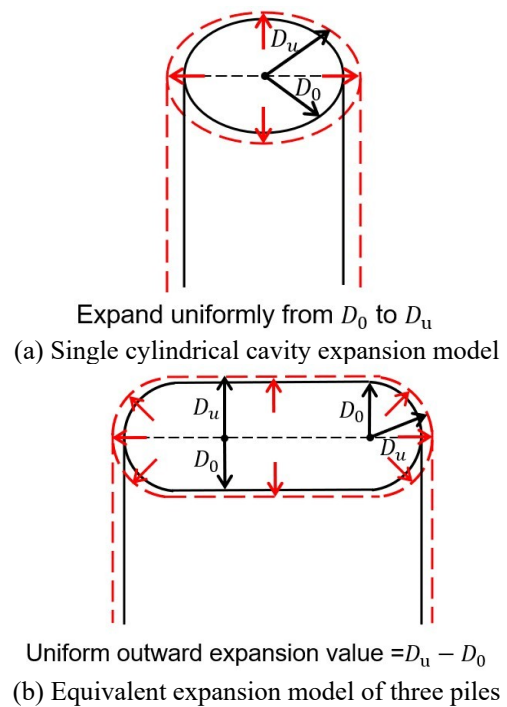


Fig. 4 Diagram of the expansion of a single cylindrical component and the equivalent simplified component of the three secant piles

the 43 m secant pile into 11 sections: ten sections of 4-meter length and one section of 3-meter length. However, due to the special construction conditions of secant piles, simplifying the construction process is crucial for efficient modeling and calculation. This study simplifies the construction of three secant piles by expanding equivalent components (shown in Fig. 4 (b)). During the calculation, uniformly expand the outer surface of the equivalent simplified component by $D_u - D_0$. The Secant piles-stratum model established in this study is depicted in Fig. 5. Fig. 5(a) shows the fundamental characteristics of the soil model and the pathway for extracting horizontal soil displacement data. Fig. 5 (b) illustrates the three specific construction scenarios analyzed in this study: a single pile, two piles, and three piles. Detailed parameter configurations for the

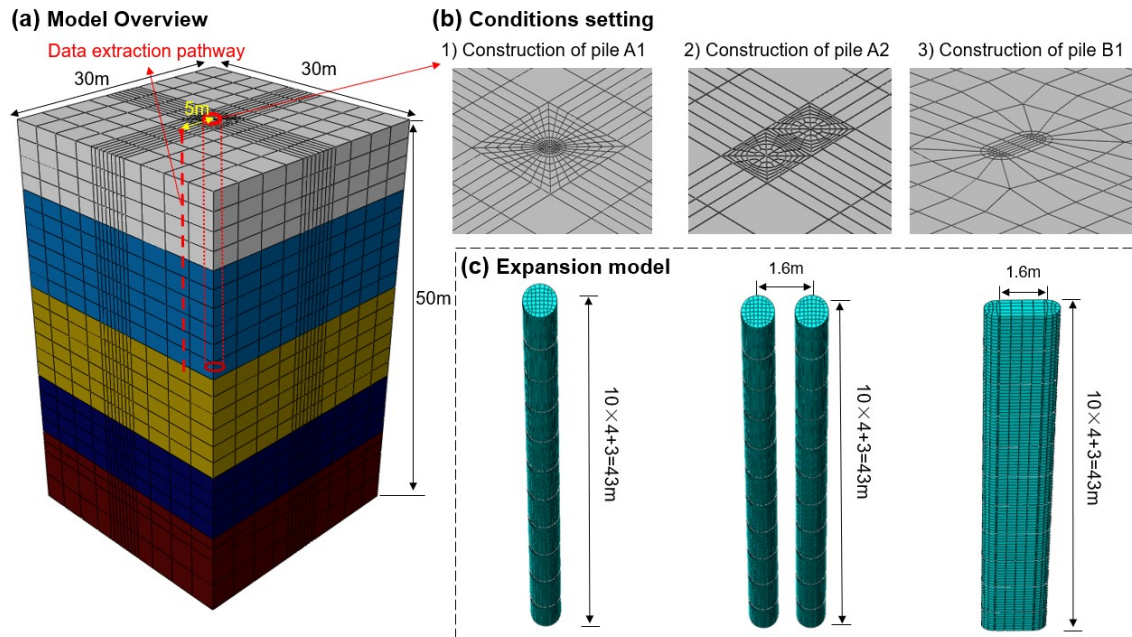


Fig. 5 Grid Settings of Secant Piles-Stratum Model and Expansion Model: (a) Model Overview, (b) Three construction conditions setting and (c) Parameter settings of expansion model

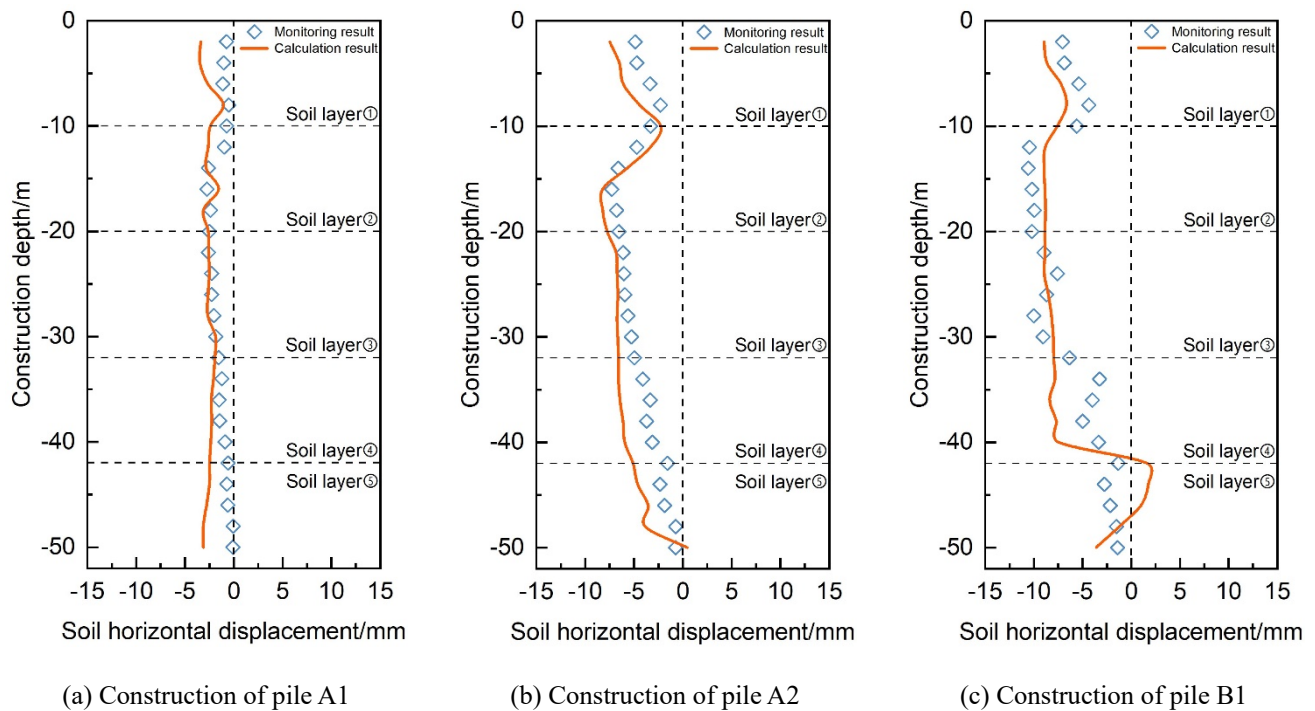


Fig. 6 Calculation results of the test pile model

expansion model under these scenarios are provided in Fig. 5(c).

4.2 Model feasibility verification

Compares the horizontal soil displacement values at a distance of 5 m from the cylindrical cavity expansion center (Fig. 5 (a)), calculated using the method described above, with the on-site measured data is shown in Fig. 6. The numerical simulation results of the trial pile demonstrate a

reasonable reflection of the soil-squeezing effect during secant pile construction. The numerical values and trends exhibit a high level of consistency, indicating that the established finite element model and the selected simplified calculation methods effectively present the soil-squeezing effects of secant pile construction in this soft soil area. These findings indicate that this approach can be utilized to conduct further research on the impact of the construction of secant piles on the deformation of adjacent existing high-speed railway bridge pile foundations.

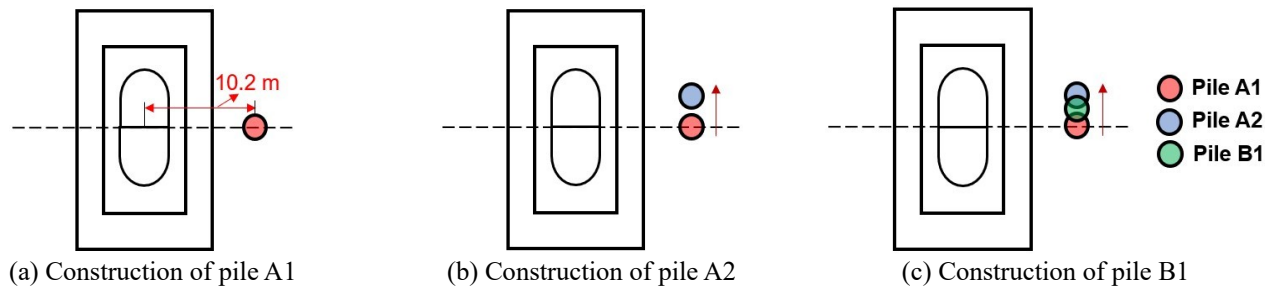


Fig. 7 Calculation condition settings for the single-side construction

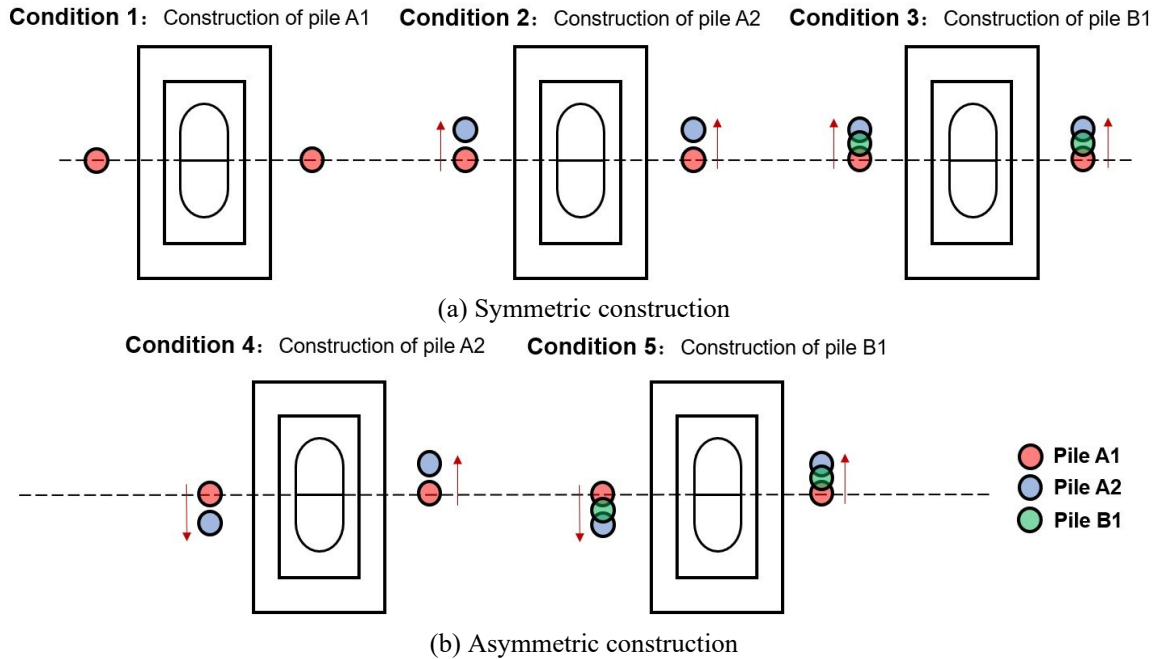


Fig. 8 Calculation condition settings for the double-sides construction

5. Influence of secant pile construction on high-speed-railway pile foundation deformation

Due to constraints such as the limited accuracy of on-site monitoring instruments and environmental factors, monitoring data regarding existing structural deformation may exhibit fluctuations, posing challenges in accurately determining deformation values and trends caused by subsequent construction activities. In practice, to accelerate construction, secant piles may be constructed simultaneously on both sides of a bridge pier, with symmetrical construction potentially involving different directions. To address these challenges and conduct more comprehensive analyses of the impact of secant pile construction on adjacent high-speed railway bridge pile foundations, this section simulates various construction scenarios. These scenarios involve the construction of secant piles on both single and double sides of the high-speed bridge pier, exploring symmetrical and asymmetrical construction conditions. The analysis focuses on the deformation characteristics of existing high-speed railway bridge pile foundations resulting from secant pile construction.

5.1 Setting of condition scenarios for calculations

The settings for the single-side construction are illustrated in Fig. 7. The center of the secant pile component is positioned 10.2 m from the center of the bridge. The settings for the double-sides construction are illustrated in Fig. 8.

5.2 Secant piles-stratum-high-speed railway bridge model

The secant piles-stratum-high-speed railway bridge model's overview is illustrated in Fig. 9. The three-dimensional finite element model dimensions are 50 m in length, 50 m in width, and 100m in height. The high-speed railway bridge pile foundation measures 63 m in length and 1.5 m in diameter, featuring two cushion caps: the upper cushion cap measures 7.4 m × 12.6 m × 2 m, and the lower cushion cap measures 10.4 m × 18.2 m × 3 m. The bridge pier is 17.5 m in height. Other material parameters, contact, and load settings in this section are the same as those in Section 4.1. Material parameter values of bridge components are consistent with secant pile components.

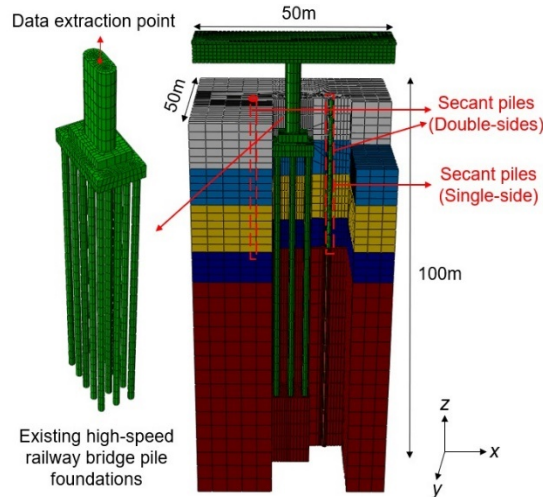
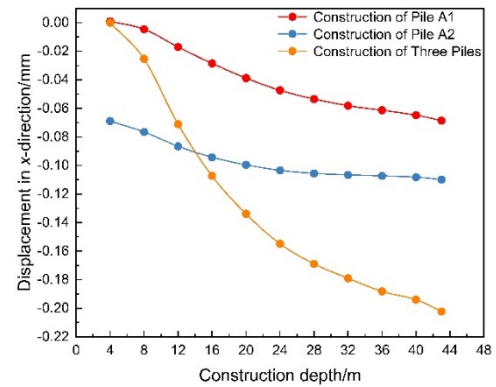


Fig. 9 Secant piles-stratum-high-speed railway bridge model

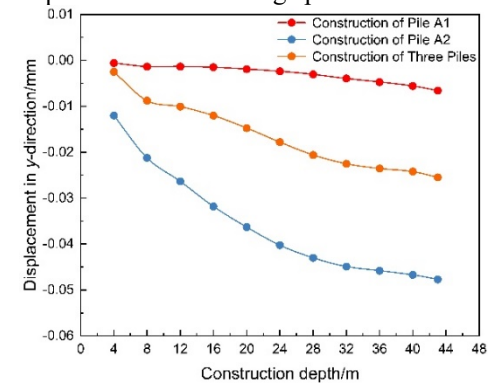
5.3 Calculation results for single-sided construction conditions

Fig. 10 illustrates the simulation results of displacement values at the top of the bridge pier under various construction conditions. The positive and negative displacements in the figures are referenced from the coordinate system shown in Fig. 9. The analysis indicates that secant pile construction predominantly affects the adjacent existing high-speed railway bridge pile foundation's deformation along the z-direction, followed by the x-direction, with the y-direction showing the least impact. As the secant pile components progressively expand along the depth, the rate of displacement growth at the pier top in the x and y-directions diminishes, while it escalates in the z-direction. Specifically, under all three construction conditions, the maximum displacement at the pier top in the x-direction is 0.2 mm, with a 0.04 mm increment after A2 pile completion and a 0.1 mm increment after B1 pile completion. This comparison highlights the greater displacement increments caused by B1 pile construction. In the y-direction, displacement calculations for the pier top range from 0.00 to -0.05 mm, indicating minimal overall impact from secant pile construction on the high-speed railway bridge pile foundation's displacement in this direction. In the z-direction, the displacement increment after A2 pile completion is 0.44 mm. However, the increment after completing the B1 pile construction reaches 2.04 mm. These data variations underscore significant difference in displacement increments between these two construction scenarios.

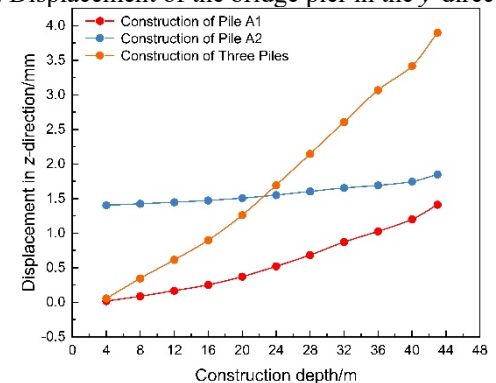
Further analysis attributes this difference to the significant influence of the simplified equivalent method for simulating the construction of three secant piles on vertical soil deformation during the soil-squeezing effect simulation, as opposed to a single pile. Additionally, the displacement in the y-direction during the construction of B1 pile is observed to be less than during the construction of A2 pile, likely because the simplified equivalent model cannot accurately replicate the sequential construction conditions of secant piles in reality.



(a) Displacement of the bridge pier in the x-direction

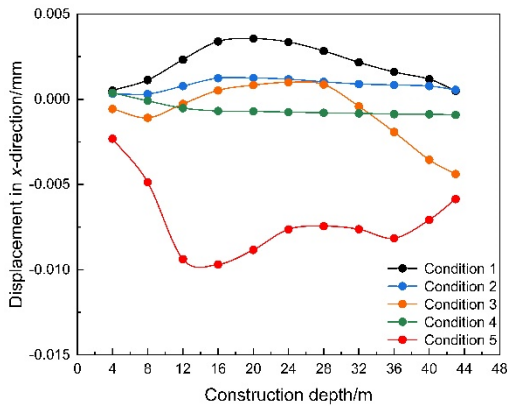


(b) Displacement of the bridge pier in the y-direction

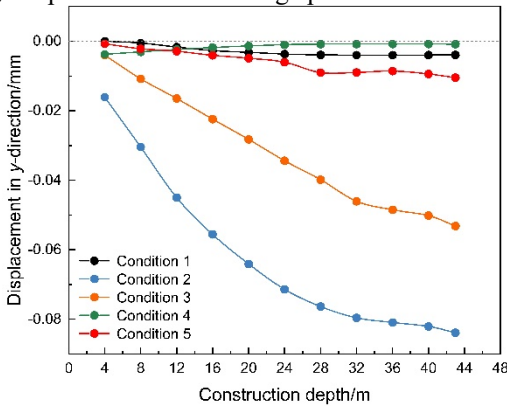


(c) Displacement of the bridge pier in the z-direction

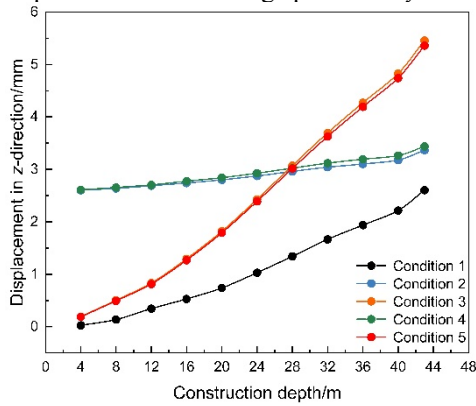
Fig. 10 Simulation results of displacement values at the top of the bridge pier (single-sided construction)



(a) Displacement of the bridge pier in the x-direction



(b) Displacement of the bridge pier in the y-direction



(c) Displacement of the bridge pier in the z-direction

Fig. 11 Simulation results of displacement values at the top of the bridge pier (double-sides construction)

5.4 Calculation results for double-sided construction conditions

The displacement results at the top of the existing high-speed railway bridge pier under double-sided construction conditions are depicted in Fig. 11. It is evident from the figure that employing asymmetric construction in the x-direction at the pier top results in notably larger displacement values. Conversely, under all conditions of symmetric construction, displacement values consistently remain within the range of 10^{-3} mm. This indicates that symmetric construction has minimal impact on x-direction displacement during actual construction. Regarding

displacement in the y-direction at the pier top, symmetrical construction shows the largest displacement values, suggesting that the arrangement of symmetrical construction induces a more pronounced soil-squeezing effect compared to asymmetrical construction. If controlling y-direction displacement is crucial during construction, avoiding symmetrical construction conditions is recommended. In terms of displacement in the z-direction, both symmetrical and asymmetrical construction conditions yield similar maximum displacement values at the top of the bridge pier. It is noteworthy that the displacement calculation results under both conditions exhibit nearly identical trends and values, indicating minimal difference between them.

6. Conclusions

This study utilizes a hybrid approach that integrates on-site test with numerical simulations. Initially, the effectiveness of the cylindrical cavity expansion method in simulating the soil-squeezing effect resulting from the construction of secant piles was validated through comparison with on-site measurement data. Building upon this foundation, we analyzed the deformation of adjacent existing high-speed railway bridge foundations under both single-sided and double-sided construction conditions of secant piles. The conclusions derived from this research are as follows:

- The analysis of on-site monitoring results indicates that the construction of scant piles in this area causes significant horizontal deformation of the surrounding soil. It is essential to enhance the monitoring of deformation in adjacent existing high-speed railway bridges. Analyzing construction parameters alongside real-time monitoring results is crucial for reducing the potential adverse effects of nearby structures.
- The simplified equivalent cylindrical cavity expansion method effectively simulates the soil-squeezing effect of three secant piles on the surrounding soil, making it suitable for disturbance calculations in analogous projects. This method is straightforward to model and exhibits high computational efficiency when implemented in practical finite element software.
- Construction of single-sided secant piles affects deformation in adjacent existing high-speed railway bridge pile foundations, primarily in the z-direction, followed by the x-direction, with the y-direction showing minimal impact. It is recommended to integrate continuous monitoring systems to track deformation in real-time, with a focus on the z-direction to mitigate risks to adjacent foundations.
- Symmetrical construction conditions exert a negligible impact on the deformation of adjacent existing high-speed railway bridge foundations in the x-direction. In contrast, symmetrical construction conditions have a more pronounced effect on deformation in the y-direction compared to asymmetrical conditions. Furthermore, both symmetrical and asymmetrical construction methods exhibit nearly identical impacts on the deformation of adjacent existing high-speed railway bridge foundations in the z-direction.

Acknowledgments

This study was supported by Natural Science Foundation of China (Grant No. 51608384). We are grateful for the anonymous referees' comments, which have improved the depth and rigor of our work.

References

- Al-Maadheedi, M.A. and Dekker, M.J. (2023), "Numerical modelling of sand plug formation during punch-through of a spudcan footing", *Ocean Eng.*, **284**, 115198. <https://doi.org/10.1016/j.oceaneng.2023.115198>.
- Bryson, L.S. and Zapata-Medina, D.G. (2010), "Finite-element analysis of secant pile wall installation", *P. I. Civil Eng.-Geotec.*, **163**(4), 209-219. <https://doi.org/10.1680/geng.2010.163.4.209>.
- Cehadeh, A., Turan, A. and Abed, F. (2015), "Numerical investigation of spatial aspects of soil structure interaction for secant pile wall circular shafts", *Comput. Geotech.*, **69**, 452-461. <https://doi.org/10.1016/j.compgeo.2015.06.014>.
- El-Nimr, M.T., Basha, A.M., Abo-Raya, M.M. and Zakaria, M.H. (2023), "Structural behavior of small-scale reinforced concrete secant pile wall", *World J. Eng.*, **20**(4), 732-745. <https://doi.org/10.1108/WJE-11-2021-0651>.
- Fall, M., Gao, Z. and Ndiaye, B.C. (2021), "Driven pile effects on nearby cylindrical and semi-tapered pile in sandy clay", *Appl. Sci-Basel.*, **11**(7), 2919. <https://doi.org/10.3390/app11072919>.
- Gao, G., Zhuang, Y., Wang, K. and Chen, L. (2019), "Influence of Benoto bored pile construction on nearby existing tunnel: A case study", *Soils Found.*, **59**(2), 544-555. <https://doi.org/10.1016/j.sandf.2018.11.006>.
- Gunawan, S., Surjandari, N.S., Setiawan, B. and Purwana, Y.M. (2022), "Horizontal movement of pile foundation due to combined loads", *Int. J. Geomate*, **22**(93), 20-27. <https://doi.org/10.21660/2022.93.j2227>.
- Jeon, Y.J. and Lee, C.J. (2023), "Analysis of pile group behaviour to adjacent tunnelling considering ground reinforcement conditions with assessment of stability of superstructures", *Geomech. Eng.*, **33**(5), 463-475. <https://doi.org/10.12989/gae.2023.33.5.463>.
- Ko, J., Jeong, S. and Lee, J.K. (2016). "Large deformation FE analysis of driven steel pipe piles with soil plugging", *Comput. Geotech.*, **71**, 82-97. <https://doi.org/10.1016/j.compgeo.2015.08.005>.
- Kumara, J.J., Kurashina, T. and Kikuchi, Y. (2016), "Effects of pile geometry on bearing capacity of open-ended piles driven into sands", *Geomech. Eng.*, **11**(3), 385-400. <https://doi.org/10.12989/gae.2016.11.3.385>.
- Liu, G.Y., Li, J.P. and Zhou, P. (2023), "Semi-analytical solution for undrained cylindrical cavity expansion in variably saturated soils", *Can. Geotech. J.*, **60**(2), 230-249. <https://doi.org/10.1139/cgj-2021-0465>.
- Lueprasert, P., Jongpradist, P., Jongpradist, P. and Schweiger, H.F. (2023), "Structural responses of a tunnel lining due to an adjacent loaded pile", *Int. J. Civ. Eng.*, **21**(6), 1027-1043. <https://doi.org/10.1007/s40999-023-00821-9>.
- Mangushev, R.A. and Nikiforova, N.S. (2023), "Technological Settlements of the surrounding buildings during the construction of deep pit fences", *Soil Mech. Found. Eng.*, **60**(1), 15-21. <https://link.springer.com/article/10.1007/s11204-023-09858-3>.
- Mittal, N., Arthur, Y.C.H. and Edwin, S.B.T. (2020), "Challenges in construction of secant bored piles in sandy soil and within a railway protection zone", *Urban Rail Transit*, **6**(2), 85-92. <https://link.springer.com/article/10.1007/s40864-019-00123-1>.
- Nguyen, A.D., Nguyen, V.T. and Kim, Y.S. (2023), "Finite element analysis on dynamic behavior of sheet pile quay wall dredged and improved seaside subsoil using cement deep mixing", *Int. J. Geo-Eng.*, **14**(1), 9. <https://doi.org/10.1186/s40703-023-00186-x>.
- Randolph, M.F., Carter, J.P. and Wroth, C.P. (1979), "Driven piles in clay - The effects of installation and subsequent consolidation", *Geotechnique*, **29**(4), 361-393.
- Rao, P.P., Li, J.P. and Zhang, C.G. (2010), "Unified solutions of cylindrical cavity expansion considering anisotropy, shear dilation and seepage", *Rock Soil Mech.*, **31**(2), 79-85.
- Sagaseta, C. (1987), "Analysis of undrained soil deformation due to ground loss", *Geotechnique*, **37**(3), 301-320.
- Shan, Y., Xiao, W.X., Ma, W.S., Liu, J.D. and Xiang, K. (2023), "Influence of developed Benoto piling on deformation of adjacent high-speed railway subgrade in soft soil area", *J. Railw. Sci. Eng.*, **20**(7), 2372-2384. <https://link.oversea.cnki.net/doi/10.19713/j.cnki.431423/u.t20221336>. (in Chinese)
- Sindhvani, A., Murthy, V.M.S.R. and Raphique, M. (2022), "Construction of rock-socketed secant piles in vicinity of heritage and high-rise buildings: Case of Mumbai metro", *Indian Geotech. J.*, **52**(2), 437-447. <https://dx.doi.org/10.1007/s40098-021-00575-y>.
- Tacim, G., Posluk, E. and Gokceoglu, C. (2023), "Importance of grouting for tunneling in karstic and complex environment (a case study from Turkiye)", *Int. J. Geo-Eng.*, **14**(1), 6. <https://doi.org/10.1186/s40703-023-00183-0>.
- Taiyari, F., Hajihassani, M. and Kharghani, M. (2022), "Efficiency of the evolutionary methods on the optimal design of secant pile retaining systems in a deep excavation", *Neural Comput. Appl.*, **34**(22), 20313-20325. <https://link.springer.com/article/10.1007/s00521-022-07591-w>.
- Vesić, A.S. (1972), "Expansion of cavities in infinite soil mass", **98**(SM3), 265-290.
- Yang, Z.X., Gao, Y.Y., Jardine, R.J., Guo, W.B. and Wang, D. (2020), "Large deformation finite-element simulation of displacement-pile installation experiments in sand", *J. Geotech. Geoenviron.*, **146**(6), 04020044. [https://doi.org/10.1061/\(ASCE\)GT.1943-5606.0002271](https://doi.org/10.1061/(ASCE)GT.1943-5606.0002271).
- Zhang, Y.M., Wang, H., Mao, J.X., Wang, F.Q., Hu, S.T. and Zhao, X.X. (2019), "Monitoring-based assessment of the construction influence of benoto pile on adjacent high-speed railway bridge: Case study", *J. Perform. Constr. Fac.*, **33**(1). [https://ascelibrary.org/doi/10.1061/\(ASCE\)CF.19435509.0001258](https://ascelibrary.org/doi/10.1061/(ASCE)CF.19435509.0001258).
- Zheng, J., Shen, M., Tu, S., Chen, Z. and Ni, X. (2024), "Investigations of countermeasures used to mitigate tunnel deformations due to adjacent basement excavation in soft clays", *Geomech. Eng.*, **36**(6), 563-573. <https://doi.org/10.12989/gae.2024.36.6.563>.
- Zhou, S., Shan, Y., Wu, Z., Zhao, W., Yang, L. and Lin, Y. (2023), "Lateral deformation of high-speed railway foundation induced by adjacent embankment construction in soft soils: Numerical and field study", *Transp. Geotech.*, **41**, 101005. <https://doi.org/10.1016/j.trgeo.2023.101005>.